Molecular mechanisms of isocitrate dehydrogenase 1 (IDH1) mutations identified in tumors: The role of size and hydrophobicity at residue 132 on catalytic efficiency

Received for publication, January 10, 2017, and in revised form, March 16, 2017 Published, Papers in Press, March 22, 2017, DOI 10.1074/jbc.M117.776179

Diego Avellaneda Matteo[‡1], Adam J. Grunseth[‡1], Eric R. Gonzalez[‡], Stacy L. Anselmo[‡], Madison A. Kennedy[‡], Precious Moman[‡], David A. Scott[§], An Hoang[‡], and Christal D. Sohl[‡2]

From the [‡]Department of Chemistry and Biochemistry, San Diego State University, San Diego, California 92182 and the [§]Sanford Burnham Prebys Medical Discovery Institute, La Jolla, California 92037

Edited by John M. Denu

Isocitrate dehydrogenase 1 (IDH1) catalyzes the reversible NADP$^+$-dependent conversion of isocitrate (ICT) to α-ketoglutarate (αKG) in the cytosol and peroxisomes. Mutations in IDH1 have been implicated in >80% of lower grade gliomas and secondary glioblastomas and primarily affect residue 132, which helps coordinate substrate binding. However, other mutations found in the active site have also been identified in tumors. IDH1 mutations typically result in a loss of catalytic activity, but many also can catalyze a new reaction, the NADPH-dependent reduction of αKG to D-2-hydroxyglutarate (D2HG). D2HG is a proposed oncometabolite that can competitively inhibit αKG-dependent enzymes. Some kinetic parameters have been reported for several IDH1 mutations, and there is evidence that mutant IDH1 enzymes vary widely in their ability to produce D2HG. We report that most IDH1 mutations identified in tumors are severely deficient in catalyzing the normal oxidation reaction, but that D2HG production efficiency varies among mutant enzymes up to ~640-fold. Common IDH1 mutations have moderate catalytic efficiencies for D2HG production, whereas rarer mutations exhibit either very low or very high efficiencies. We then designed a series of experimental IDH1 mutants to understand the features that support D2HG production. We show that this new catalytic activity observed in tumors is supported by mutations at residue 132 that have a smaller van der Waals volume and are more hydrophobic. We report that one mutation can support both the normal and neomorphic reactions. These studies illuminate catalytic features of mutations found in the majority of patients with lower grade gliomas.

Metabolic changes in tumors have been described for nearly a century (1–3), but only relatively recently have enzymes involved in metabolic processes been established as tumor suppressors or oncoproteins. One of the more striking examples of metabolic enzymes playing a role in tumorigenesis includes isocitrate dehydrogenase 1 and 2 (IDH1 and IDH2).[3] These homodimeric enzymes are responsible for the reversible NADP$^+$- and Mg^{2+}-dependent conversion of ICT to αKG (Fig. 1*A*) in the cytosol and peroxisomes (IDH1), or mitochondria (IDH2). IDH3 is responsible for the same reaction within the context of the TCA cycle, although the oxidative decarboxylation catalyzed by this enzyme is non-reversible and NAD$^+$-dependent.

Mutations in IDH1 and IDH2 were identified in glioblastoma multiforme in a large sequencing effort (4), and soon >80% of adult grade II/III gliomas and secondary glioblastomas were found to have IDH1 mutations, commonly R132H or R132C IDH1 (5, 6) (reviewed in Refs. 7–9). Subsequently ~10–20% of acute myeloid leukemias were shown to have primarily IDH2 mutations, typically R140Q or R172K IDH2 (10). Early mechanisms of tumorigenesis focused on deficient conversion of ICT to αKG (11), suggesting that IDH serves as a tumor suppressor, in part through altering levels of hypoxia-inducible transcription factor-1α (12). However, IDH1 and IDH2 mutations appeared heterozygously in tumors, an unusual feature of a tumor suppressor. In landmark studies (13–15), the most common IDH1 and IDH2 mutations were shown to catalyze a neomorphic reaction: the Mg^{2+}- and NADPH-dependent reduction of αKG to D2HG (Fig. 1*B*). This suggested IDH1 and IDH2 likely encode for oncoproteins. D2HG is proposed to be an oncometabolite; it competitively inhibits αKG-dependent enzymes including the TET family of 5-methylcytosine hydroxylases and the JmjC family of histone lysine demethylases, resulting in cell de-differentiation (16, 17). Indeed, cancer patients with IDH mutations display hypermethylated phenotypes (18–20) resulting from D2HG-mediated inhibition of histone and DNA demethylation. The proposed oncometabolite D2HG alone can recapitulate tumorigenic phenotypes in cancer models (21, 22), but studies measuring global metabolomics changes between mutant IDH1 expression and D2HG treatment show some differences (23, 24), indicating loss of the

This work was supported by National Institute of Health Grants K99 CA187594 (to C. D. S.), R00 CA187594 (to C. D. S.), 5T34 GM008303 (to E. R. G. and M. A. K.), and P30 CA030199 (to D. A. S.), a Summer Undergraduate Research Program Grant from San Diego State University (to M. A. K.), and San Diego State University startup funds (to C. D. S.). The authors declare that they have no conflicts of interest with the contents of this article. The content is solely the responsibility of the authors and does not necessarily represent the official views of the National Institutes of Health.
This article contains supplemental Figs. S1–S6.

[1] Both authors contributed equally to this work.
[2] To whom correspondence should be addressed: CSL 328, MC1030, 5500 Campanile Dr., San Diego, CA 92182. Tel.: 619-594-2053; Fax: 619-594-4634; E-mail: csohl@mail.sdsu.edu.

[3] The abbreviations used are: IDH, isocitrate dehydrogenase; ICT, isocitrate; αKG, α-ketoglutarate; D2HG, D-2-hydroxyglutarate; AML, acute myeloid leukemia.

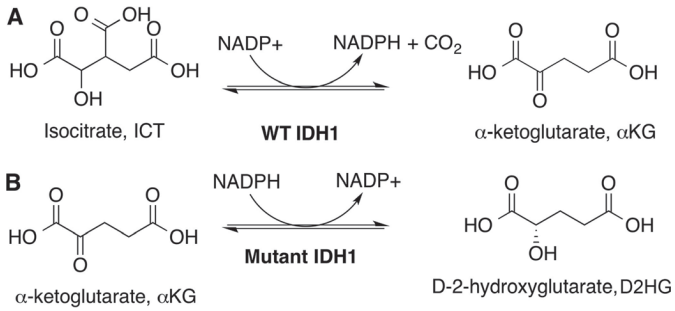

Figure 1. WT and mutant IDH1 catalytic activities. Shown are the: *A,* normal oxidative decarboxylation, and *B,* the neomorphic reduction.

normal reaction and/or altered NADPH levels may also play an important role. Development of selected targeted therapy against oncogenic IDH1 and IDH2 mutations is underway and results are promising (8).

A point mutation conferring a new catalytic activity suggests important mechanistic features, and many have used kinetics and structural methods to explore mutant IDH1 and IDH2 activity (13, 25–30). There is evidence that IDH1 mutations produce varying concentrations of D2HG (30), with somewhat subtle but interesting alterations in conformational changes as shown in crystal structures of R132H IDH1 (26, 27, 29). In general, reported kinetic parameters of IDH1 mutants explored to date vary widely, making comparisons difficult. Interestingly, some mutations identified in tumors do not appear to generate D2HG (31, 32), suggesting that loss of the normal reaction itself has important consequences, or perhaps that they are simply passenger mutations.

Here we report a thorough catalytic study of a wide spectrum of IDH1 mutations, including many identified in tumors and several mutants designed to clarify catalytic features. We show that IDH1 mutants vary widely in catalytic efficiency, with more polar and larger residues at position 132 supporting the normal reaction, and more hydrophobic and smaller residues driving the neomorphic reaction. These findings provide significant insight into the types of mutations that may be accommodated at residue 132 for efficient D2HG production. By determining the catalytic features of IDH1 mutations, we reveal features of driver mutations present in the majority of patients with lower grade gliomas and secondary glioblastomas.

Results

Structural modeling and thermal stability of IDH1 mutations

For the mutations explored in this work, only structures of WT and R132H IDH1 in complex with both substrates (ICT and $NADP^+$, or αKG and $NADP^+$) have been reported (13, 27, 29, 33), although a recent high resolution cryo-EM structure shows R132C IDH1 in complex with NADPH (34). To help inform the structural consequences of R132C, R132G, R100Q, A134D, and H133Q IDH1, these mutants were modeled in previously solved structures of R132H IDH1 in complex with αKG, $NADP^+$, and Ca^{2+} (Protein Data Bank (PDB) 4KZO (27)) and WT IDH1 in complex with ICT, $NADP^+$, and Ca^{2+} (PDB 1T0L (33)) using the geometry minimization package in Phenix (35). These models were then aligned to the original structures using PyMOL (36) (Fig. 2). In both models, minimal global changes

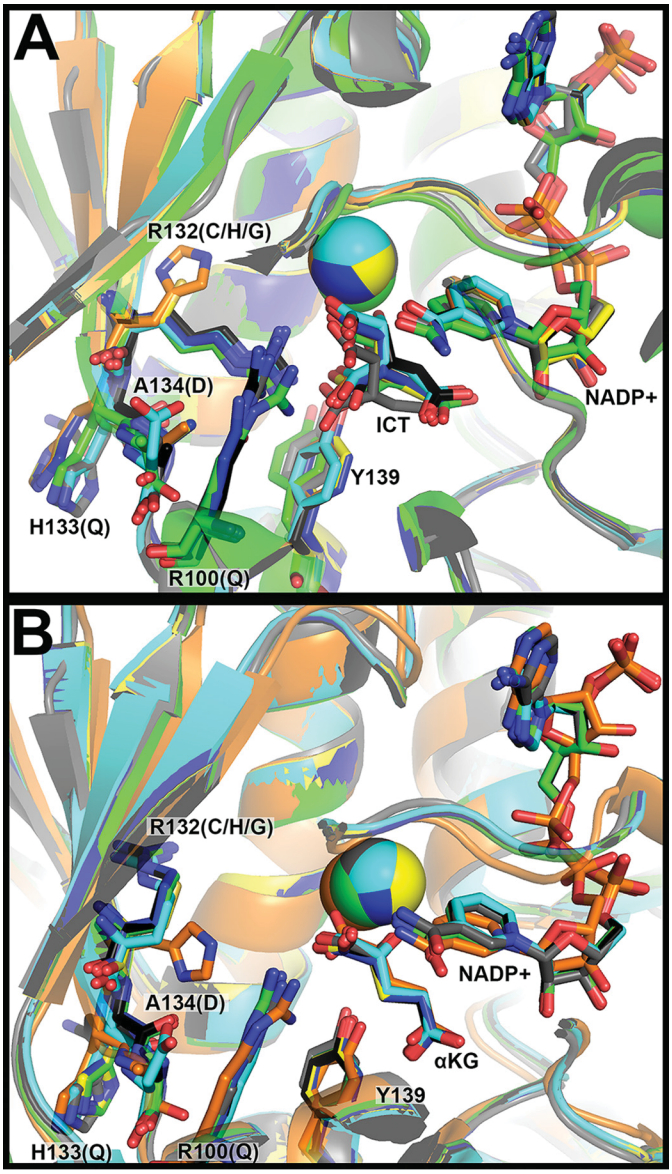

Figure 2. Structural modeling of IDH1 mutations identified in tumors. *A,* the structure of WT IDH1 complexed with ICT, $NADP^+$, and Ca^{2+} (PDB 1T0L (33)) and *B,* R132H IDH1 complexed with αKG, $NADP^+$, and Ca^{2+} (PDB 4KZO (27)) were used to model additional mutations. In both panels, WT IDH1 is shown in *green*, A134D in *cyan*, H133Q in *black*, R100Q in *dark blue*, R132H in *orange*, R132C in *yellow*, and R132G in *gray*. Substrates and residues that are mutated are highlighted in *stick format*, as well as catalytic residue Tyr-139. Ca^{2+} is shown as a *sphere*. Ligand restraint generation and optimization of provided cif files were generated using eLBOW in the Phenix software suite (35), and mutations were made using Coot (54). Geometry Minimization (Phenix software suite) (35) was used to regularize geometries of the models, with 500 iterations and 5 macro cycles.

were identified, consistent with previous structural work on R132H IDH1. The presence of the C3 carboxylate in ICT requires some adjustment of the catalytic residue Tyr-139, whereas less movement of this residue is seen in the models containing αKG.

To explore the mechanistic features of these IDH1 mutations identified in tumors, cDNA constructs were generated for heterologous expression and purification in *Escherichia coli.* WT, R132H, R132C, R132G, R100Q, A134D, and H133Q IDH1 homodimers were expressed and purified to >95% purity

(supplemental Fig. S1*A*). Thermal stability was assessed for each enzyme using circular dichroism to perform thermal shift assays. The melting temperature (T_m) of each of the IDH1 mutants varied little compared with WT IDH1 (supplemental Fig. S2A). R132C IDH1 had the lowest T_m (46.8 °C), but this represents only a 5% change from WT IDH1 (T_m = 49.1 °C). R100Q IDH1 had the highest T_m (51.9 °C), again signifying only a 5% change from WT IDH1.

Efficiency of reactions catalyzed by IDH1 mutants found in tumors

The most common IDH1 mutations found in gliomas are R132H followed by R132C (37). R132G, which has been identified with higher frequency in chondrosarcomas (38, 39), is less frequently seen in gliomas and is a known D2HG producer (30). R100Q IDH1, a long predicted D2HG producer based on the R140Q IDH2 mutation affecting the identical residue, is relatively rare (40). A134D and H133Q IDH1 are rare mutations found in thyroid cancers and are predicted to only be deficient in the normal reaction (31, 40). Steady-state kinetic assays were used to determine the catalytic efficiency of the conversion of ICT to αKG (normal reaction) by monitoring the production of NADPH at $A_{340\ nm}$, or αKG to D2HG (neomorphic reaction) by monitoring the consumption of NADPH, at both 21 and 37 °C. All mutants were deficient in the normal reaction, ranging from a relatively minor 3.5-fold loss of catalytic efficiency (k_{cat}/K_m) for H133Q IDH1, whereas the other mutations exhibited more severe ~300- to 1,340-fold losses in efficiency (Fig. 3, supplemental Fig. S3, Table 1). The observed changes in catalytic efficiency are driven both by decreases in k_{cat} and increases in K_m.

Mutants varied widely in their relative catalytic efficiency of D2HG production (Fig. 4, supplemental Fig. S4, Table 2). Only rate-saturating concentrations of substrates generated rates of D2HG production above the signal-to-noise threshold for A134D IDH1 and H133Q IDH1. Thus only upper limits of k_{cat} values are reported as k_{obs} (Fig. 4, *B* and *D*) because K_m values could not be obtained. R132G IDH1 is the most efficient producer of D2HG (~125-fold more efficient than WT IDH1), driven primarily by low K_m values but also by a high k_{cat}. R132C and R132H IDH1 are ranked next in catalytic efficiency, with a low K_m value reported for R132C IDH1 (Table 2). This suggests that production of D2HG in tumors by R132G and R132C IDH1 may be more significant than R132H IDH1 when cytosolic concentration of αKG is considered. This trend is supported by D2HG measurements in glioma tissue (30). Due to its high K_m, R100Q IDH1 was one of the least efficient producers of D2HG (Table 2).

GC/MS analysis confirms D2HG production by IDH1 tumor mutants

Although the normal reaction is reversible (Fig. 1*A*), a lower pH and source of CO_2 (typically $NaHCO_3$) are required to favor the reverse reaction *in vitro*, and work by Leonardi *et al.* (25) have shown that the reverse reaction is deficient in IDH1 mutants. Regardless, we desired to confirm that the less well characterized IDH1 mutants, namely R100Q and R132G, favor D2HG production over ICT when incubated with αKG and NADPH. R132H and R132C IDH1 are well established to produce D2HG (first reported in Ref. 13, but confirmed by many groups). Gas chromatography/mass spectrometry (GC/MS) was used to identify and quantify the amount of D2HG as well as αKG and ICT (not shown) produced in these incubations (Fig. 5) (20). R132G IDH1 gave robust production of D2HG consistent with kinetic data, whereas an incubation with R100Q IDH1 showed D2HG production levels near the lower limit of detection, again consistent with kinetic findings (Figs. 4 and 5). Levels of ICT for both mutants were <0.1 nmol, based on limits of detection. This indicates that NADPH oxidation in the presence of αKG is preferably coupled to D2HG production under these reaction conditions. This also supports previous findings that both mutants generate D2HG in *in vitro* assays (30). These experiments do not necessarily indicate that the reverse of the normal reaction is ablated, however, as pH < 7 and CO_2 are required for this reaction *in vitro* (25).

Generation of IDH1 mutants engineered to explore mechanistic features of D2HG production

In addition to R132H/R132C/R132G IDH1, several rarer IDH1 mutations in gliomas have been identified, including R132S/R132L/R132V IDH1 (5, 6, 41, 42). *In vitro* kinetic assays have shown that R132S and R132L IDH1 catalyze production of D2HG at rates similar to the more common R132H and R132C IDH1 mutations (13, 25). Similarly, ectopic expression of R132S and R132L IDH1 in HEK293T cells indicate D2HG production levels are comparable with cell lines expressing R132C and R132H IDH1 (30). R132H/R132C/R132G/R132S/R132L/R132V IDH1 all vary in the degree of hydrophobicity at residue 132, and all have a smaller van der Waals volume than the wild-type arginine. Although these clues illuminate interesting mechanistic characteristics of R132H IDH1, the features that allow IDH1 mutants to generate D2HG with varying catalytic efficiency are not fully clear.

We designed several IDH1 mutations to serve as tools to probe the limits of hydrophobicity (43) and van der Waals volume (44) at residue 132 that support D2HG production. R132A IDH1 is truly an engineered mutation, as to our knowledge it has not been identified in tumors. This residue serves as an example of a more hydrophobic and smaller residue at position 132, similar to R132G IDH1. R132A IDH1 has been shown to be deficient in the normal reaction (29), but its ability to catalyze the neomorphic reaction has not yet been explored. R132N IDH1 also has not been identified in tumors to date. Asparagine has a much smaller van der Waals volume than arginine, although the ranked polarities of these two amino acids are similar. R132Q IDH1 plays an important role in driving chondrosarcomas and a small number of gliomas, and mouse mR132Q IDH1 generates D2HG about 20-fold more efficiently than human R132H IDH1 *in vitro* (39, 45). This mutation has the most similar ranking in hydrophobicity as compared with WT, but a smaller van der Waals volume. R132K IDH1 is homologous to R172K IDH2, one of the most common D2HG-producing mutations seen in acute myeloid leukemia (11, 41). However, R132K IDH1 has not been reported in tumors, and the activity of this enzyme has not been assessed. R132K IDH1 is most comparable with WT IDH1 when considering both van der Waals volume and polarity ranking of residue 132. Finally,

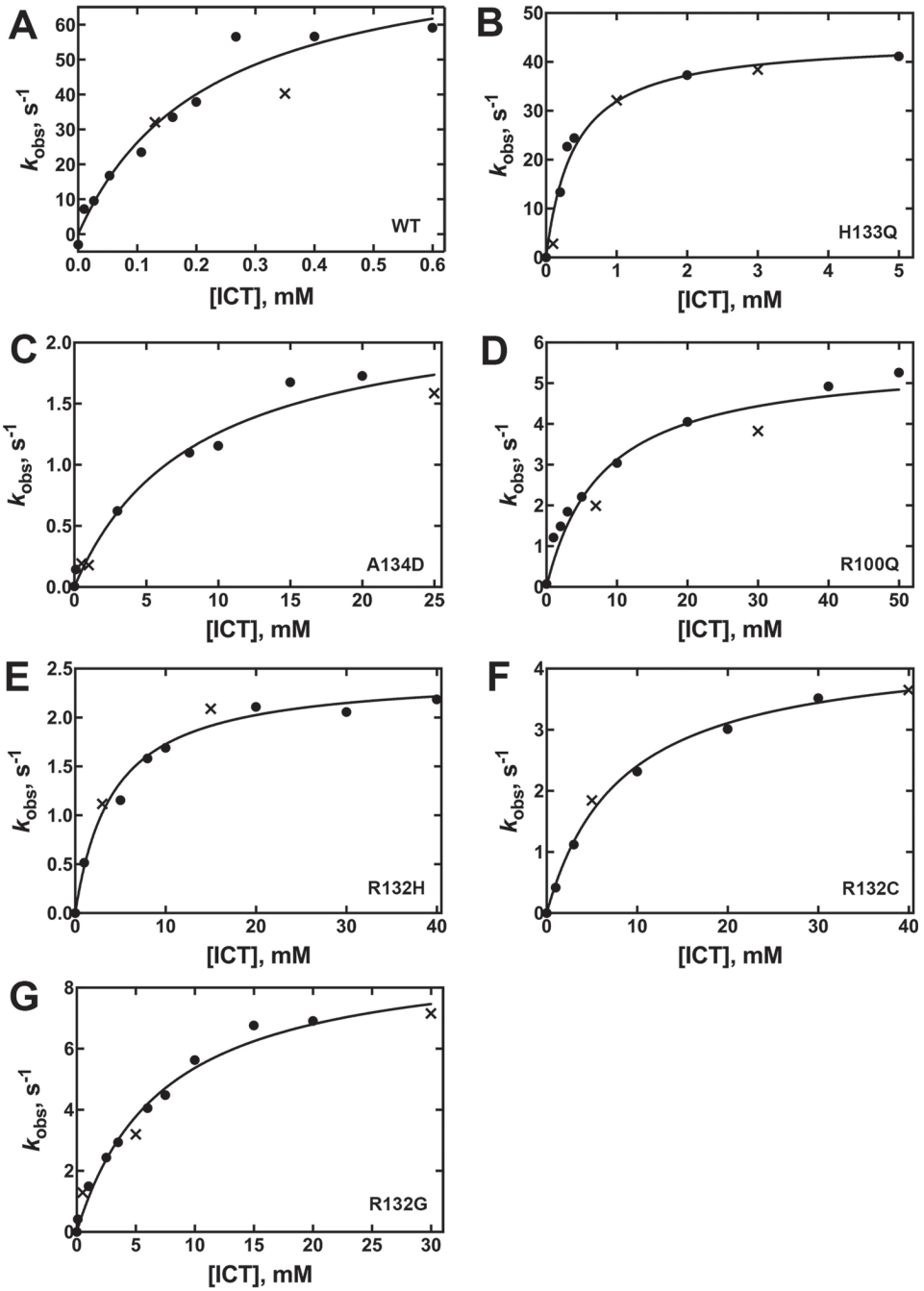

Figure 3. Concentration dependence of the ICT concentration on the observed rate of NADPH production in the normal reaction (37 °C). The determined k_{obs} values were obtained from two different enzyme preparations to ensure reproducibility. The k_{obs} values resulting from each of the two enzyme preparations are distinguished by using either a *circle* or an × in the plots. The observed rate constants (k_{obs}) were calculated from the linear range of the slopes of plots of concentration *versus* time using GraphPad Prism software (GraphPad, San Diego, CA). These k_{obs} values were then fit to a hyperbolic equation to generate k_{cat} and K_m values, and the standard error listed in Table 1 results from the deviance from these hyperbolic fits is indicated. The determined k_{obs} values were obtained from two different enzyme preparations to ensure reproducibility. Results from assays at 21 °C are shown in supplemental Fig. S3. *A,* WT IDH1. *B,* H133Q IDH1. *C,* A134D IDH1. *D,* R100Q IDH1. *E,* R132H IDH1. *F,* R132C IDH1. *G,* R132G IDH1.

R132W IDH1 is another example of an engineered mutation in that it has not been identified in tumors. It was selected to represent the most extreme case of a large van der Waals volume coupled with high hydrophobicity.

Structural modeling and thermal stability of engineered IDH1 mutations

Because no crystal structures of these mutants are currently available, each was modeled in a previously solved structure of R132H IDH1 in complex with αKG, $NADP^+$, and Ca^{2+} (PDB code 4KZO (27)) using the geometry minimization package in Phenix (35) followed by alignment in PyMOL (36) (Fig. 6). Few changes are observed globally or within the active site. The size of the amino acid at position 132 does necessitate some local adjustments to avoid steric hindrance, but overall, changes in the models are minimal.

All five IDH1 mutants were successfully heterologously expressed and purified to >95% purity (supplemental Fig. S1*B*).

Table 1
Kinetic parameters for the normal reaction, conversion of ICT to αKG, catalyzed by IDH1
Values result from fits of kinetic data using two different enzyme preparations. The standard error is determined from the deviance from these hyperbolic fits (Fig. 3, supplemental Fig. S3).

IDH1	Relative hydrophobicity of residue 132[a]	van der Waals volume of side chain at residue 132, Å^3 [b]	k_{cat} (37 °C)	$K_{m,ICT}$ (37 °C)	$K_{m,NADP+}$ (37 °C)	Efficiency, ($k_{cat}/K_{m,ICT}$, 37 °C)	k_{cat} (21 °C)	$K_{m,ICT}$ (21 °C)	$K_{m,NADP+}$ (21 °C)	Efficiency, mM^{-1} s^{-1} ($k_{cat}/K_{m,ICT}$, 21 °C)
			s^{-1}	mM		$mM^{-1}\,s^{-1}$	s^{-1}	mM		$mM^{-1}\,s^{-1}$
WT	−14 (R)	148 (Arg)	85 ± 4	0.22 ± 0.02	0.08 ± 0.03	$3.9 \pm 0.4 \times 10^2$	11.0 ± 0.4	0.015 ± 0.003	0.03 ± 0.01	$7.3 \pm 1.3 \times 10^2$
H133Q	−14 (Arg)	148 (Arg)	45 ± 2	0.40 ± 0.08	0.16 ± 0.02	$1.1 \pm 0.2 \times 10^2$	9.4 ± 0.6	0.28 ± 0.07	0.101 ± 0.008	35 ± 9
A134D	−14 (Arg)	148 (Arg)	2.3 ± 0.2	8 ± 2	1.2 ± 0.3	0.29 ± 0.08	0.200 ± 0.008	2.7 ± 0.3	0.7 ± 0.1	0.074 ± 0.003
R100Q	−14 (Arg)	148 (Arg)	5.6 ± 0.4	8 ± 2	0.18 ± 0.02	0.7 ± 0.2	1.40 ± 0.06	9 ± 1	0.070 ± 0.006	0.16 ± 0.02
R132H	8 (His)	118 (His)	2.4 ± 0.1	4.2 ± 0.6	1.6 ± 0.5	0.57 ± 0.08	0.120 ± 0.006	6 ± 1	1.0 ± 0.9	0.020 ± 0.003
R132C	49 (Cys)	86 (Cys)	4.4 ± 0.1	8.2 ± 0.8	0.75 ± 0.07	0.54 ± 0.05	1.61 ± 0.08	5.3 ± 0.8	0.58 ± 0.08	0.30 ± 0.05
R132G	0 (Gly)	48 (Gly)	9.3 ± 0.6	7 ± 1	0.067 ± 0.007	1.3 ± 0.2	1.0 ± 0.06	3.6 ± 0.6	0.14 ± 0.02	0.28 ± 0.05

[a] From Ref. 43.
[b] From Ref. 44.

Thermal stability was assessed using circular dichroism in thermal shift assays. Again, minimal changes were observed in T_m (supplemental Fig. S2*B*). R132K IDH1 had the highest T_m (49.8 °C), which varied from WT IDH1 by only 2%.

Kinetic analysis of engineered IDH1 mutants

The catalytic efficiency of the normal reaction was measured for all mutants, and efficiencies were plotted against relative hydrophobicity according to Monera *et al.* (43) (Fig. 7*A*), and against van der Waals volume (44) (Fig. 7*B*). All mutants were significantly deficient in converting ICT to αKG, driven both by a decrease in k_{cat} as well as an increase in K_m (Table 3, supplemental Fig. S5). Two IDH1 mutations maintained moderate oxidative decarboxylation activity; R132Q and R132K IDH1 had 33- and 56-fold losses of αKG production efficiency relative to WT IDH1, respectively. All other mutations had ≥220-fold decreases in catalytic efficiency.

IDH1 mutants were also incubated with αKG and NADPH to measure presumptive D2HG production efficiency (Fig. 7, Table 4, supplemental Fig. S6). R132Q IDH1 was the most efficient D2HG producer of the mutants explored in this work, with 4-fold higher efficiency than the next most efficient mutant, R132G IDH1. There was a notable decrease in efficiency in all other mutants, with R132A IDH1 having similar catalytic efficiencies as R132G/R132C/R132H IDH1. R132N/R132K/R132W and WT IDH1 were all very poor at producing D2HG. The severely deficient catalytic efficiency seen in R132N IDH1 was primarily driven by a very high K_m value (Table 4). This suggests that like R100Q IDH1, D2HG production by R132N IDH1 may not be physiologically relevant when the cytosolic concentration of αKG is considered. Relative efficiencies of the other mutants were driven both by changes in k_{cat} and K_m, with a low K_m value driving R132A IDH1 production (Table 4).

GC/MS analysis confirms D2HG production by engineered IDH1 mutants

To confirm that an incubation of the engineered IDH1 mutants with αKG and NADPH favors D2HG production rather than the reverse of the normal reaction (*i.e.* ICT production), GC/MS was used to quantify levels of D2HG, ICT, and αKG of the engineered IDH1 mutants. Measured amounts of D2HG were as expected under the incubation lengths at experimentally measured kinetic efficiency. R132Q and R132G IDH1 generated the highest levels of D2HG (Fig. 5), followed by R132A IDH1. Again, levels of ICT were difficult to measure due to their very low concentrations (<0.1 nmol, based on limits of detection). This suggests that NADPH oxidation is coupled primarily to D2HG production, rather than ICT, under these experimental conditions.

Discussion

Here we report the first in-depth, simultaneous catalytic characterization of 11 IDH1 mutations and WT IDH1, including mutations identified in tumors (R132H/R132C/R132G/R132Q, R100Q, A134D, and H133Q IDH1) and additional mutations (R132A/R132K/R132N/R132W IDH1) designed to measure the effects of hydrophobicity (43) and van der Waals

DOCKET ALARM

Explore Litigation Insights

Docket Alarm provides insights to develop a more informed litigation strategy and the peace of mind of knowing you're on top of things.

Real-Time Litigation Alerts

Keep your litigation team up-to-date with **real-time alerts** and advanced team management tools built for the enterprise, all while greatly reducing PACER spend.

Our comprehensive service means we can handle Federal, State, and Administrative courts across the country.

Advanced Docket Research

With over 230 million records, Docket Alarm's cloud-native docket research platform finds what other services can't. Coverage includes Federal, State, plus PTAB, TTAB, ITC and NLRB decisions, all in one place.

Identify arguments that have been successful in the past with full text, pinpoint searching. Link to case law cited within any court document via Fastcase.

Analytics At Your Fingertips

Learn what happened the last time a particular judge, opposing counsel or company faced cases similar to yours.

Advanced out-of-the-box PTAB and TTAB analytics are always at your fingertips.

API

Docket Alarm offers a powerful API (application programming interface) to developers that want to integrate case filings into their apps.

LAW FIRMS
Build custom dashboards for your attorneys and clients with live data direct from the court.

Automate many repetitive legal tasks like conflict checks, document management, and marketing.

FINANCIAL INSTITUTIONS
Litigation and bankruptcy checks for companies and debtors.

E-DISCOVERY AND LEGAL VENDORS
Sync your system to PACER to automate legal marketing.